Eur. J. Mineral.
2018, **30**, 835–840
Published online 4 May 2018

Description and crystal structure of vanderheydenite, $Zn_6(PO_4)_2(SO_4)(OH)_4{\cdot}7H_2O$, a new mineral from Broken Hill, New South Wales, Australia

PETER ELLIOTT[1,2,*] and UWE KOLITSCH[3,4]

[1]Department of Earth Sciences, School of Physical Sciences, The University of Adelaide, Adelaide, South Australia 5005, Australia
*Corresponding author, e-mail: peter.elliott@adelaide.edu.au
[2] South Australian Museum, North Terrace, Adelaide, South Australia 5000, Australia
[3]Mineralogisch-Petrographische Abt., Naturhistorisches Museum, Burgring 7, 1010 Wien, Austria
[4] Institut für Mineralogie und Kristallographie, Universität Wien, Althanstraße 14, 1090 Wien, Austria

Abstract: Vanderheydenite, $Zn_6(PO_4)_2(SO_4)(OH)_4{\cdot}7H_2O$, is a new mineral from the Block 14 Opencut, Broken Hill, New South Wales, Australia. It occurs as aggregates of colourless crystals up to 0.5 mm across in voids of a sphalerite–galena matrix and is associated with anglesite, pyromorphite, sulfur, and liversidgeite. Crystals are pseudohexagonal blades up to 0.4 mm in length, flattened on {1 0 0} and exhibiting the forms {1 0 0}, {0 1 0}, and {0 2 1}. Cleavage was not observed. The Mohs hardness is estimated to be 3. The calculated density is 3.12 g/cm^3 from the empirical formula and 3.06 g/cm^3 from the ideal formula. The mineral is optically biaxial (–), with $\alpha = 1.565(4)$, $\beta = 1.580(4)$ and $\gamma = 1.582(4)$. The calculated $2V$ is 39.8°. Chemical analysis by electron microprobe gave ZnO 55.63, CuO 0.07, FeO 0.11, MnO 0.06, P_2O_5 14.18, As_2O_5 4.33, SO_3 8.71, H_2O 18.31, total 101.40 wt%, with H_2O content derived from the refined crystal structure. The empirical formula calculated on the basis of 23 oxygen atoms is $(Zn_{5.99}Cu_{0.01}Fe_{0.01}Mn_{0.01})_{\Sigma 6.02}[(PO_4)_{1.75}(AsO_4)_{0.33}]_{\Sigma 2.08}(SO_4)_{0.95}(OH)_{3.91}{\cdot}6.96H_2O$. The mineral is monoclinic, $P2_1/n$, with $a = 6.2040(12)$, $b = 19.619(4)$, $c = 7.7821(16)$ Å, $\beta = 90.67(3)°$, $V = 947.1(3)$ Å^3. The five strongest lines in the X-ray powder diffraction pattern are [d(Å), (I), (hkl)]: 9.826 (57) (0 2 0), 7.296 (20) (0 1 1), 6.134 (1 0 0) (0 2 1), 3.368 (10) (0 3 2, 1 5 0), 3.069 (9) (2 1 0, 0 4 2). The crystal structure of vanderheydenite ($R1 = 0.0497$ for 939 reflections with $F_o > 4\sigma F$) contains chains of edge-sharing ZnO_6 octahedra parallel to a that are linked by edge- and corner-sharing ZnO_5 trigonal bipyramids and TO_4 (T = P, As) tetrahedra forming zig-zag sheets parallel to {0 1 0}. Sheets are linked by half-occupied, distorted TO_4 (T = P, S) tetrahedra in the [0 1 1] direction. Interstitial channels extend parallel to the a-direction and are occupied by strongly to weakly hydrogen-bonded H_2O groups.

Key-words: vanderheydenite; new mineral; zinc phosphate sulfate; crystal structure; Broken Hill; New South Wales; Australia.

1. Introduction

The Broken Hill mines in western New South Wales, Australia have been major source of Pb and Zn ores since the late 19th century and are well known for the diversity and spectacular appearance of their minerals (Birch, 1999). The deposit is the type locality for 21 mineral species. Vanderheydenite is a new mineral found in a specimen collected in 1999 from sulphide ore stockpiles mined from the Block 14 Opencut, Broken Hill, which had been dumped at the Pinnacles Mine, 15 km south west of Broken Hill for processing. Vanderheydenite has been approved by the Commission of New Minerals, Nomenclature and Classification of the IMA (2014-076). The mineral is named in honour of Arnold van der Heyden who worked as a mine geologist at Broken Hill for the former Minerals Mining and Metallurgy Ltd from December 1985 until June 1991. The name is in recognition of his contribution to the understanding of the secondary mineralogy of the Broken Hill ore body by the systematic collecting of mineral specimens from the oxidized zone (Birch & van der Heyden, 1988, 1997). The holotype specimen is deposited in the South Australian Museum, Adelaide, South Australia (registration number G32512). This specimen is also the holotype specimen for liversidgeite, $Zn_6(PO_4)_4 \cdot 7H_2O$ (Elliott *et al.*, 2010).

2. Occurrence

The Broken Hill ore body consists of massive, recrystallised sphalerite- and galena-rich sulphide hosted within a unit of gneiss known as the Potosi Gneiss. The orebody has an extensive oxidized zone that is noted for its mineralogical diversity, which has resulted from the chemical complexity of the sulphide mineralization and its host rocks, and a long history of weathering and oxidation (Birch, 1990, 1999). The lower portion of the oxidized zone grades into silver-rich supergene mineralization, comprising coronadite, quartz, kaolinite, and goethite (Van der Heyden & Edgecombe, 1990). Between this and the sulphide zone is an

0935-1221/18/0030-2750 $ 2.70
https://doi.org/10.1127/ejm/2018/0030-2750

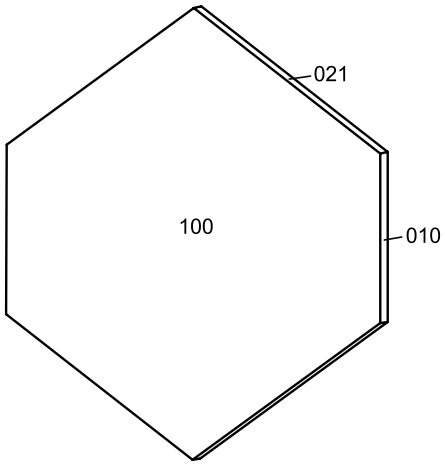

Fig. 1. Crystal drawing (SHAPE V7.1.2, Shape Software 2004) showing a bladed pseudohexagonal crystal of vanderheydenite.

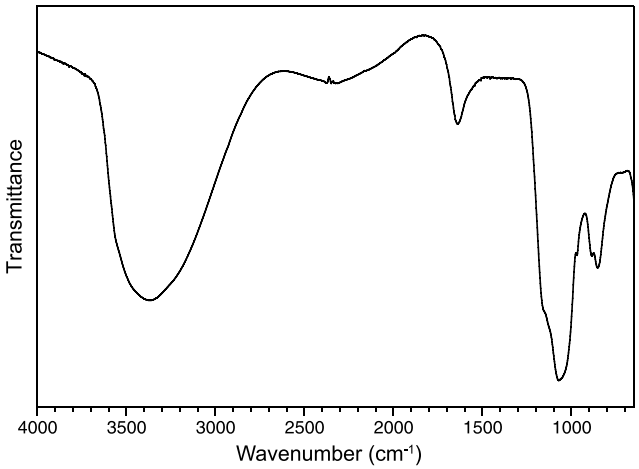

Fig. 2. The FT-IR spectrum of powdered vanderheydenite.

irregular zone of cerussite, whose boundary with the sulphide zone is marked by a band of leached sulphides. The specimen containing vanderheydenite came from this zone of highly weathered sulphide ore in the Block 14 Opencut and comprises leached, coarse-grained sphalerite and galena with minor chalcopyrite, quartz, and fluorapatite. The new mineral formed in cavities as a result of the release of Zn, S, As and P from the breakdown of sphalerite, galena, and fluorapatite; the source of the As is most likely arsenopyrite which is present in minor amounts in sphalerite–galena ore at Broken Hill. Associated minerals are colourless to white prisms of pyromorphite, colourless crystals of anglesite, and aggregates of colourless to white crystals of liversidgeite.

3. Appearance, physical and optical properties

Vanderheydenite occurs as aggregates of colourless crystals up to 0.5 mm across. Individual crystals are thin blades that are flattened on {1 0 0} and are up to 0.4 mm in width and 0.05 mm in thickness. Crystal forms are major {1 0 0}, {0 1 0}, and {0 2 1}, resulting in a pseudohexagonal outline (Fig. 1). Vanderheydenite has a white streak and a vitreous lustre; it does not fluoresce under ultraviolet light. Cleavage was not observed. The Mohs hardness is estimated to be 3 and the mineral is brittle with an uneven fracture. The density was not measured due to the paucity of material. The calculated density is 3.12 g/cm^3 from the empirical formula and 3.06 g/cm^3 from ideal formula. The indices of refraction (white light) are $\alpha = 1.565(4)$, $\beta = 1.580(4)$, $\gamma = 1.582(4)$; $2V$ was not measured, $2V$ (calc.) = 39.8°. The Gladstone-Dale relationship gives a compatibility index of 0.059, rated as good (Mandarino, 1981).

Table 1. Compositional data for vanderheydenite.

Constituent	Weight%	Range	Standard deviation
ZnO	55.63	54.49–56.68	0.65
CuO	0.07	0.00–0.21	0.08
FeO	0.11	0.00–0.28	0.10
MnO	0.06	0.00–0.15	0.06
P_2O_5	14.18	13.10–15.29	0.63
As_2O_5	4.33	3.14–5.18	0.58
SO_3	8.71	7.31–9.85	0.81
H_2O*	18.31		
Total	101.40		

Note: Number of analyses = 13.
* calculated from the structural formula taking into account charge-balance.

4. Infrared spectroscopy

The infrared spectrum (Fig. 2) of powdered vanderheydenite in the range 4000–650 cm^{-1} was obtained using a Nicolet 5700 FTIR spectrometer equipped with a Nicolet Continuum IR microscope and a diamond-anvil cell. The spectrum shows bands due to OH stretching vibrations (a broad band at ~3674 to ~2720 cm^{-1}, centred around 3368 cm^{-1}), H–O–H bending of H_2O groups (ν_2, at 1636 cm^{-1}), ν_3 vibration of the SO_4 tetrahedra, overlapping with ν_3 vibration of the PO_4 tetrahedra (1056 cm^{-1}), ν_1 vibration of the SO_4 tetrahedra, overlapping with ν_1 vibration of the PO_4 tetrahedra (at 968 cm^{-1}) and ν_1 and ν_3 vibrations of the AsO_4 tetrahedra (at 885 and 853 cm^{-1}).

5. Chemical analysis

Vanderheydenite was analysed using a Cameca SX51 electron microprobe operating in wavelength-dispersive mode with an accelerating voltage of 15 kV, a specimen current of 10 nA and a beam diameter of 10 µm (Table 1). The following standards and X-ray lines were used for calibration: chalcopyrite (Cu$K\alpha$, S$K\alpha$), sphalerite (Zn$K\alpha$), almandine (Fe$K\alpha$, Al$K\alpha$), rhodonite (Mn$K\alpha$), GaAs (As$L\alpha$), and hydroxylapatite (P$K\alpha$). No additional element with atomic number ≥9 was detected in amounts >0.05 wt% oxide. Data were reduced using the φ(ρZ) method of Pouchou & Pichoir (1985). As only a small amount of material was available, a direct water determination was not carried out, but the presence of H_2O was confirmed by both

Table 2. X-ray powder diffraction data for vanderheydenite.

I_{obs}	d_{obs}	I_{calc}	d_{calc}	h	k	l	I_{obs}	d_{obs}	I_{calc}	d_{calc}	h	k	l
57	9.826	38	9.810	0	2	0	8	2.432	9	2.439	2	0	$\bar{2}$
20	7.296	14	7.233	0	1	1			17	2.433	2	5	0
100	6.134	100	6.096	0	2	1	5	2.515	5	2.516	1	5	$\bar{2}$
2	5.922	3	5.915	1	1	0	8	2.411	22	2.421	2	1	$\bar{2}$
1	5.252	3	5.243	1	2	0			27	2.412	2	0	2
2	4.848	3	4.905	0	4	0			10	2.411	0	3	3
		3	4.823	1	0	1			10	2.394	2	1	2
5	4.715	9	4.734	1	1	$\bar{1}$	8	2.342	23	2.366	1	1	3
4	4.368	10	4.328	1	2	1	5	2.284	17	2.274	0	$\bar{7}$	$\bar{2}$
2	4.156	9	4.149	0	4	$\bar{1}$	1	2.258	5	2.256	1	$\bar{3}$	$\bar{3}$
1	3.900	8	3.910	1	3	$\bar{1}$	1	2.342	10	2.366	1	1	3
		8	3.848	1	4	0	2	2.284	23	2.274	0	7	2
10	3.368	21	3.344	0	3	2	1	2.191	5	2.191	$\bar{8}$	$\bar{1}$	$\bar{1}$
		3	3.316	1	5	0	1	2.178	3	2.184	2	4	$\bar{2}$
9	3.069	3	3.064	2	1	0	1	2.104	3	2.099	0	9	1
		21	3.048	0	4	2	1	2.081	4	2.079	2	7	0
3	3.025	10	3.015	0	6	$\bar{1}$	1	2.045	4	2.049	1	$\bar{5}$	$\bar{3}$
1	2.960	16	2.956	1	3	$\bar{2}$	1	2.014	5	2.013	2	$\bar{7}$	$\bar{1}$
1	2.897	3	2.893	1	6	0	1	1.969	4	1.962	0	10	0
2	2.858	9	2.862	2	1	$\bar{1}$			10	1.961	2	2	$\bar{3}$
5	2.807	3	2.803	2	3	0	1	1.949	10	1.939	2	2	3
8	2.778	19	2.763	0	5	2	1	1.786	5	1.784	2	9	0
		10	2.754	2	2	1	1	1.752	15	1.743	0	5	4
8	2.648	11	2.646	2	3	$\bar{1}$	1	1.713	3	1.707	2	6	$\bar{3}$
		10	2.637	0	7	1							
		11	2.628	2	3	1							

Note: Calculated intensities were obtained using the program LAZY PULVERIX (Yvon *et al.*, 1977); only reflections with $I_{calc} > 3$ were considered.

crystal-structure solution and infrared spectroscopy (Fig. 2). The empirical formula was calculated on the basis of 23 oxygen atoms, giving $(Zn_{5.99}Cu_{0.01}Fe_{0.01}Mn_{0.01})_{\Sigma 6.02}[(PO_4)_{1.75}(AsO_4)_{0.33}]_{\Sigma 2.08}(SO_4)_{0.95}(OH)_{3.91}\cdot 6.96H_2O$. The ideal formula is $Zn_6(PO_4)_2(SO_4)(OH)_4\cdot 7H_2O$.

6. X-ray powder-diffraction

Powder X-ray diffraction data (Table 2) were collected using a Rigaku Hiflux Homelab diffractometer (Cu$K\alpha$ X-radiation, $\lambda = 1.541870$ Å). Calculated intensities were obtained from the structural model using the program UNITCELL (Holland & Redfern, 1997). Unit-cell parameters refined using the Le Bail profile-fitting method (Le Bail *et al.*, 1988; Hunter, 1998) and starting from the unit-cell parameters determined from the single-crystal study, are $a = 6.209(2)$, $b = 19.637(7)$, $c = 7.822(3)$ Å, $\beta = 90.672(2)°$, $V = 953.64(6)$ Å^3. These values show good agreement with the single-crystal ones.

7. Structure determination

7.1. Single-crystal X-ray data collection and structure solution

Single-crystal X-ray intensity data were collected using a crystal $0.07 \times 0.05 \times 0.005$ mm in size on an Oxford Diffraction Xcalibur E diffractometer equipped with an Eos CCD detector using Mo$K\alpha$ X-radiation ($\lambda = 0.71073$ Å) and a detector distance of 46.5 mm. Data collection conditions are given in Table 3. The data were processed using the CrysAlisPro program (Oxford Diffraction, 2009) and corrected for Lorentz and polarization effects. An empirical absorption correction was applied using the SCALE3 ABSPACK algorithm, as implemented in CrysAlisPro. E-statistics ($|E^2-1| = 0.982$) indicated a centrosymmetric space group and systematic absences were compatible with space group $P2_1/n$. The structure was solved by direct methods using SHELXS-97 (Sheldrick, 2008) within the WinGX program suite (Farrugia 2012) and refined using SHELXL-97 (Sheldrick, 2008). An unambiguous location of H atoms in difference-Fourier maps could not be obtained. The refinement with anisotropic factors converged at $R_1 = 0.0497$ for 939 independent reflections with $F_o > 4\sigma(F)$. Fractional coordinates and atom displacement parameters are provided in Table 4, selected interatomic distances in Table 5, and bond valences (Brese & O'Keeffe, 1991) are given in Table 6.

7.2. Structure description

The crystal structure of vanderheydenite contains three Zn sites. Refined occupancies are 0.983(10) and 0.988(8) for the Zn1 and Zn2 sites respectively, which both contain minor Fe, Mn and Cu in addition to Zn, and 0.99(2) for the

Table 3. Crystal data, data-collection and refinement details for vanderheydenite.

Crystal data	
Formula	$Zn_6(PO_4)_2(SO_4)(OH)_4{\cdot}7H_2O$
Space group	$P2_1/n$
a, *b*, *c* (Å)	6.2040(12), 19.619(4), 7.7821(16)
β (°)	90.67(3)
V (Å^3), Z	947.1(3), 2
F(000)	784.9
μ (mm^{-1})	7.45
Absorption correction	multi-scan, T_{min}, T_{max} = 0.78, 1.00
Crystal dimensions (mm)	0.07 × 0.05 × 0.005
Data collection	
Diffractometer	Oxford Diffraction Xcalibur E
Temperature (K)	293
Radiation	Mo*K*α, λ = 0.71073 Å
θ range (°)	2.62–26.73
Detector distance (mm)	46.5
Rotation axes	ω
Rotation width	1.0
Total no. of frames	350
Collection time per frame (s)	23.26
h, k, l ranges	$\overline{7} \rightarrow 7$, $\overline{22} \rightarrow 24$, $\overline{9} \rightarrow 9$
Total reflections measured	6195
Unique reflections	1920 (R_{int} = 0.0907)
Total no. of frames	
Refinement	
Refinement on	F^2
$R1$* for $F_0 > 4\sigma(F_0)$	4.97%
$wR2$† for all F_0^2	12.28%
Reflections used $F_0^2 > 4\sigma(F_0^2)$	939
Number of parameters refined	164
Extinction factor	0.0000(6)
(Δ/σ)max	0.000
$\Delta\rho_{min}$, $\Delta\rho_{max}$ (e/Å^3)	−0.954, 1.453
GooF	0.727

* $R1 = \Sigma||F_o|-|F_c||/\Sigma|F_o|$

† $wR2 = \Sigma w(|F_o|^2-|F_c|^2)^2/\Sigma w|F_o|^2)^{1/2}$; $w = 1/[\sigma^2(F_o^2) + (0.042\,P)^2 + 12.60\,P]$; $P = ([\text{max of } (0 \text{ or } F_o^2)] + 2\,F_o^2)/3$

Zn3 site. The Zn1 and Zn2 sites are each coordinated by three O^{2-} anions, two OH groups, and one H_2O group in regular octahedral coordinations. The Zn3 site is coordinated by three O^{2-} anions and two OH groups in a distorted trigonal bipyramid, with Zn3–O bond lengths ranging between 1.967(7) and 2.124(8) Å. The structure contains two *T* sites, each coordinated by four O atoms in a tetrahedral arrangement. The TO_4 tetrahedra show different degrees of geometrical distortion. The $T1O_4$ (*T*1 = P, As; see below for details) tetrahedron has a fairly regular geometry, with *T*1–O bond distances of 1.542(8)–1.567(7) Å and O–*T*1–O angles 107.5(4) to 112.4(4)°. The $T2O_4$ (*T*1 = P, S) group consists of two half-occupied distorted tetrahedral groups [refined P occupancy 0.408 (10)] sharing a common O6–O6 edge with a *T*2–*T*2 distance of 2.012(13) Å. The apical O atom (O5), a ligand of only *T*2, at 1.457(17) Å, is also half occupied [refined occupancy of 0.48(2)]. The $T2O_4$ tetrahedron has two short *T*2–O bond distances of 1.457(17) and 1.503(10) Å and two long distances of 1.565(10) and 1.608(11) Å, with $\langle T1\text{–O}\rangle$ = 1.533 Å. The O–*T*2–O angles vary from 99.5(6) to 120.9(6)° (mean 109.3°). The results of the structure refinement suggest that there is distinct ordering of P, As, and S in the *T* sites. The refined site occupancy for the *T*1 site (18.06 *epfu*) indicates that As is present at this site. This is also supported by $\langle T1\text{–O}\rangle$ = 1.559 Å. The refined occupancy ($P_{0.83}As_{0.17}$) is in good agreement with the chemical analysis. The $\langle T2\text{–O}\rangle$ distance (1.533 Å) indicates that S is present at this site. In agreement with the chemical-analytical data, the occupancy of the *T*2 site was fixed to $S_{0.47}P_{0.03}$ which improved the structural model. Half-occupancy of *T*2 results in two environments around O7. When the one half of *T*2 is present, its O7 ligand is bonded to Zn2 and *T*2, while the other, symmetrically equivalent half (*T*2') is then vacant and its O7 ligand is bonded only to Zn2, so represents H_2O (the local addition of two hydrogen atoms to form H_2O is needed to achieve charge balance). Thus, on average, the O7 site is an "OH". Due to this half-occupancy, all O ligands of *T*2 (O5, O6, O7) have U_{eq} values about twice as high as those of the other O ligands.

The crystal structure of vanderheydenite is comprised of zig-zag sheets of $Zn\varphi_6$ octahedra, $Zn\varphi_5$ trigonal bipyramids and TO_4 tetrahedra. Alternate $Zn1\varphi_6$ (φ = O, OH, or H_2O) and $Zn2\varphi_6$ octahedra share *trans* edges to form a $[M\varphi_4]$ chain that extends parallel to [1 0 0] (Figs. 3, 4) The $Zn3\varphi_5$ trigonal bipyramids share an edge with both $Zn1\varphi_6$ and $Zn2\varphi_6$ octahedra and link to a second $[M\varphi_4]$ chain by corner sharing, forming zig-zag sheets in the (0 1 0) plane. Sheets are decorated by corner-sharing $T1O_4$ tetrahedra. Sheets link in the [0 1 1] direction by $T2O_4$ tetrahedra which share corners with $Zn1\varphi_6$ and $Zn2\varphi_6$ octahedra. Interstitial channels between the sheets extend parallel to the *a*-direction and are occupied by H_2O groups (OW11 and OW12), which are strongly to weakly hydrogen-bonded (for details see below). The H_2O groups show some positional disorder, as evidenced by their anisotropic displacement ellipsoids (Table 4).

The H atoms were not located in the refinement, however, OH and H_2O groups were identified by the bond-valence distributions in the structure (Table 6). OH8 and OH9 (1.21 and 1.17 valence units, *vu*, respectively), which are each bonded to three Zn cations, are OH groups. OW10, OW11, and OW12 (0.47, 0, and 0 *vu*, respectively) are H_2O molecules. While OW10 is a ligand of Zn1, OW11 and OW12 occupy interstitial channels which run between the sheets along the *a*-direction. As mentioned previously, when the one half of the *T*2 site is unoccupied, the O7 atom (then bonded only to the Zn2 site) represents an H_2O molecule. The average bond-valence sum of the O7 atom is (1.50 + 0.33)/2 = 0.915 *vu*. Based on stereochemical considerations and O...O distances, O5 likely accepts a hydrogen bond from OH8, and OW11 is a likely acceptor atom of hydrogen bonds from both OH9 and OW10. OW12 is a likely acceptor atom of hydrogen bonds from OH8 and OW10. The implied hydrogen bonds are of medium strong to weak strength, with O...O distances in the range of 2.694–2.999 Å. There is more ambiguity concerning the positions of H atoms associated with

Table 4. Fractional coordinates and displacement parameters (Å^2) for atoms for vanderheydenite.

	Mult.	*x*	*y*	*z*	U_{eq}	U_{11}	U_{22}	U_{33}	U_{12}	U_{13}	U_{23}
Zn1	4	0.38570(19)	0.14364(7)	0.82044(16)	0.0117(5)	0.0089(8)	0.0143(9)	0.0119(8)	0.0010(6)	−0.0003(6)	0.0016(6)
Zn2	4	0.8824(2)	0.14255(7)	0.81668(16)	0.0127(5)	0.0085(8)	0.0184(9)	0.0112(8)	0.0014(6)	−0.0029(6)	−0.0010(6)
Zn3	4	0.6349(2)	0.21976(7)	0.52393(18)	0.0126(5)	0.0092(7)	0.0176(9)	0.0109(7)	0.0034(6)	−0.0011(6)	0.0000(7)
*T*1	4	0.6316(3)	0.22806(12)	0.1331(3)	0.0085(8)	0.0064(13)	0.0134(15)	0.0056(11)	0.0002(9)	−0.0026(9)	−0.0014(11)
*T*2	4	0.6298(10)	0.0084(3)	0.9267(8)	0.012(2)	0.005(3)	0.015(4)	0.016(4)	−0.001(3)	−0.002(3)	0.004(3)
O1	4	0.6151(13)	0.1810(4)	0.2911(9)	0.032(2)	0.032(5)	0.052(6)	0.012(4)	−0.001(4)	−0.005(4)	−0.007(4)
O2	4	0.8382(11)	0.2733(4)	0.1443(9)	0.029(2)	0.029(5)	0.031(5)	0.025(5)	−0.011(4)	−0.008(4)	−0.002(4)
O3	4	0.6371(11)	0.1872(4)	−0.0399(9)	0.024(2)	0.013(4)	0.036(5)	0.023(5)	−0.004(4)	−0.004(4)	0.006(4)
O4	4	0.4307(11)	0.2765(4)	0.1336(9)	0.022(2)	0.026(4)	0.019(5)	0.022(4)	−0.003(4)	0.001(3)	0.000(4)
O5	4	0.624(3)	−0.0227(10)	0.757(2)	0.041(7)	0.040(12)	0.062(16)	0.020(10)	−0.015(9)	0.005(9)	0.010(11)
O6	4	0.4051(15)	0.0484(5)	0.9470(12)	0.051(3)	0.064(7)	0.043(6)	0.045(6)	0.016(5)	0.011(5)	0.018(5)
O7	4	0.8498(14)	0.0472(4)	0.9401(12)	0.048(3)	0.047(6)	0.033(6)	0.064(7)	0.029(5)	−0.012(5)	−0.011(5)
OH8	4	0.6344(11)	0.1255(4)	0.6580(9)	0.022(2)	0.016(4)	0.035(5)	0.016(4)	0.000(4)	−0.003(4)	−0.001(4)
OH9	4	0.1311(10)	0.1772(4)	0.9621(8)	0.0170(19)	0.009(4)	0.026(5)	0.016(4)	0.003(3)	0.002(4)	0.005(3)
OW10	4	0.1362(12)	0.0912(4)	0.6578(10)	0.031(2)	0.025(4)	0.036(5)	0.033(5)	−0.005(4)	−0.002(4)	−0.003(4)
OW11	4	0.8269(16)	−0.1304(7)	0.6865(14)	0.089(5)	0.068(8)	0.159(12)	0.040(7)	0.022(8)	−0.016(6)	−0.064(8)
OW12	4	0.220(2)	−0.0441(5)	0.6390(13)	0.080(4)	0.160(12)	0.028(7)	0.050(7)	−0.003(5)	−0.030(8)	0.004(7)

Note: The anisotropic displacement factors (U_{ij}) are defined as $\exp[-2\pi^2\Sigma^3_{i=1}\Sigma^3_{\phi=1}3j U_{ij}a_i^* a_j^* h_i h_j]$

Table 5. Selected interatomic distances (Å) for vanderheydenite.

Zn1–OH8	2.038(7)	Zn2–OH8	1.990(7)
Zn1–OH9	2.045(7)	Zn2–OH9	2.021(7)
Zn1–O3	2.075(7)	Zn2–O3	2.090(7)
Zn1–O6	2.116(9)	Zn2–O7	2.114(8)
Zn1–O2	2.148(7)	Zn2–O4	2.157(7)
Zn1–OW10	2.238(8)	Zn2–OW10	2.252(8)
⟨Zn–O⟩	2.110	⟨Zn–O⟩	2.104
Zn3–O1	1.967(7)	*T*1–O1	1.542(8)
Zn3–O4	2.016(7)	*T*1–O2	1.560(7)
Zn3–OH9	2.079(7)	*T*1–O3	1.567(7)
Zn3–O2	2.080(8)	*T*1–O4	1.567(7)
Zn3–OH8	2.124(8)	⟨*T*–O⟩	1.559
⟨Zn–O⟩	2.053		
*T*2–O5	1.457(17)		
*T*2–O6	1.503(10)		
*T*2–O7	1.565(10)		
*T*2–O6	1.608(11)		
⟨*T*–O⟩	1.533		

Table 6. Bond-valence analysis for vanderheydenite.

	Zn1	Zn2	Zn3	*T*1	*T*2	Sum
O1			0.49	1.33		1.82
O2	0.30		0.36	1.26		1.92
O3	0.37	0.35		1.24		1.96
O4		0.29	0.43	1.24		1.96
O5					1.57	1.57
O6[1]	0.33				1.39↓→ 1.04↓	1.72
O7[2]		0.33			1.17	1.50
O7[3]		0.33				0.33
OH8	0.41	0.46	0.32			1.19
OH9	0.40	0.43	0.36			1.19
OW10	0.24	0.23				0.47
OW11						0.00
OW12						0.00
Sum	2.05	2.09	1.97	5.07	5.17	

[1] Valence sum for the O6 site is based on 50% occupancy of the *T*2 site.
[2] O7 bonded to Zn2 and *T*2
[3] O7 bonded only to Zn2
[4] Bond-valence sum for the *T*1 site is based on the occupancy $P1_{0.832(9)}As1_{0.168(9)}$

OW11 and OW12. Possible hydrogen-bond receptors in the vicinity of OW11 are O1, O5, OH9, OW10, and OW12. Potential donor–acceptor distances in the range 2.913–2.973 Å and possible hydrogen-bond receptors in the vicinity of OW12 are O1, O5, OH8, OW10, and OW11 with potential donor–acceptor distances in the range 2.931–2.973 Å. Each of these atoms seems favored as receptors because of their incident bond-valence deficiency (Table 6). The O1, O6, and O7 anions show incident bond-valence deficiencies, however, there are no nearby OH or OW atoms that do not represent polyhedral edges.

8. Discussion

Vanderheydenite is chemically and structurally unique. There are five hydrated Zn phosphate minerals (including liversidgeite that has a stoichiometrically similar formula, $Zn_6(PO_4)_4 \cdot 7H_2O$) and nine hydrated Zn sulfate minerals. Several minerals contain both phosphate and sulfate groups, however, vanderheydenite is the first Zn phosphate sulfate mineral. The $[MT\varphi_4]$ chains of edge-sharing octahedra are found as a fundamental building block in a wide variety of oxysalt mineral structures. Chains are usually decorated by tetrahedral oxyanions in a staggered arrangement on either side of the chain along its length. Chains can be isolated or can polymerize to form octahedron-tetrahedron linked sheets or octahedron-tetrahedron linked heteropolyhedral frameworks. Linkage of chains by both tetrahedra and trigonal bipyramids to form zig-zag sheets as in vanderheydenite is unique among mineral structures.

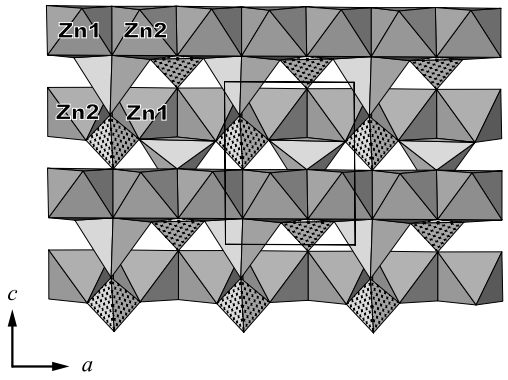

Fig. 3. The crystal structure of vanderheydenite viewed along [0 1 0]. Znφ$_6$ octahedra are dark grey; Zn3φ$_5$ trigonal bipyramids are pale grey; *T*1O$_4$ tetrahedra are cross-shaded (*T*2O$_4$ tetrahedra are not visible in this view). Water molecules are omitted. The unit cell is outlined. All structure drawings were done with ATOMS (Dowty, 1999).

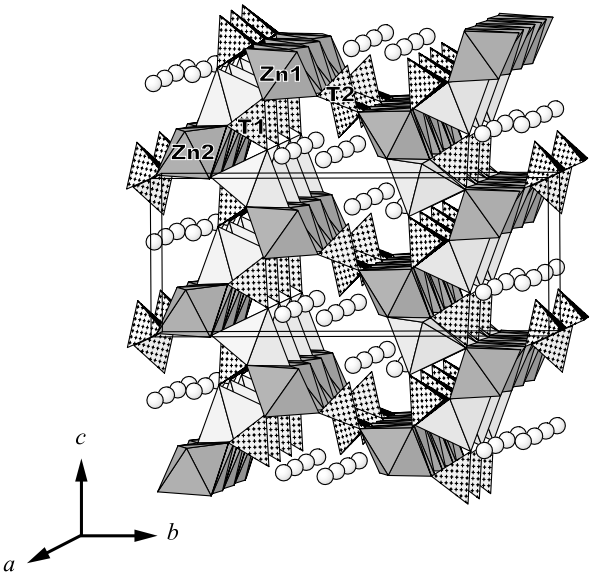

Fig. 4. The crystal structure of vanderheydenite in a view slightly offset from the [1 0 0] direction. Znφ$_6$ octahedra are dark grey; Zn2φ$_5$ trigonal bipyramids are pale grey; *T*O$_4$ tetrahedra are cross-shaded; H$_2$O groups are white circles. The unit cell is outlined.

Acknowlegements: The authors thank the staff of Adelaide Microscopy, The University of Adelaide, especially Angus Netting, for assistance with the electron-microprobe analysis. We also thank Mark Cooper for preliminary single-crystal X-ray investigations of vanderheydenite. The infrared spectrum was obtained with the assistance of the Forensic Science Centre, Adelaide. The paper benefited from comments by two anonymous reviewers.

References

Birch, W.D. (1990): Minerals from the Kintore and Block 14 opencuts, Broken Hill, N.S.W; review of recent discoveries, including tsumebite, kipushite and otavite. *Aust. Mineral.*, **5**, 125–141.

Birch, W.D. (1999): The Minerals. *in* Minerals of Broken Hill, W.D. Birch, ed. Broken Hill Council, Broken Hill. 88–256.

Birch, W.D. & van der Heyden, A. (1988): Minerals of the Kintore Opencut, Broken Hill, New South Wales. *Min. Rec.*, **19**, 425–436.

—, — (1997): Minerals from the Kintore and Block 14 Open cuts, Broken Hill, New South Wales. *Aust. J. Mineral.*, **3**, 23–71.

Brese, N.E. & O'Keeffe, M. (1991): Bond-valence parameters for solids. *Acta Cryst.*, **B47**, 192–197.

Dowty, E. (1999): ATOMS for Windows and Macintosh. Version 5.0.6. Shape Software, Kingsport, Tennessee, USA.

Elliott, P., Giester, G., Libowitzky, E., Kolitsch, U. (2010): Description and crystal structure of liversidgeite, $Zn_6(PO_4)_4 \cdot 7H_2O$, a new mineral from Broken Hill, New South Wales, Australia. *Am. Mineral.*, **95**, 397–404.

Farrugia, L.J. (2012): WinGX and ORTEP for *Windows*: an update. *J. Appl. Crystallogr.*, **45**, 849–854.

Hawthorne, F.C. (1992): Bond topology, bond-valence and structure stability, *in* "The Stability of Minerals". G.D. Price and N.L. Ross, ed. Chapman & Hall, London, 25–87.

Hawthorne, F.C. (1998): Structure and chemistry of phosphate minerals. *Mineral. Mag.*, **62**, 141–164.

Holland, T.J.B. & Redfern, S.A.T. (1997): Unit cell refinement from powder diffraction data: the use of regression diagnostics. *Mineral. Mag.*, **61**, 65–77.

Hunter, B.A. (1998): Rietica – A Visual Rietveld Program. Commission on Powder Diffraction Newsletter, **20**, 21.

Le Bail, A., Duroy, H., Fourquet, J.L. (1988): Ab-initio structure determination of $LiSbWO_6$ by X-ray powder diffraction. *Mater. Res. Bull.*, **23**, 447–452.

Mandarino, J.A. (1981): The Gladstone-Dale relationship: Part IV: The compatibility concept and its application. *Can. Mineral.*, **19**, 441–450.

Oxford Diffracton (2009): CrysAlis PRO. Oxford Diffraction Ltd, Yarnton, England.

Pouchou, J.L. & Pichoir, F. (1985): "PAP" φ (ρZ) procedure for improved quantitative microanalysis. *in* "Microbeam Analysis", J.T. Armstrong, ed. San Francisco Press, California, 104–106.

Shape Software (1997): ATOMS for Windows and Macintosh V 4.0, Kingsport, Tennessee, USA.

Sheldrick, G.M. (2008): A short history of *SHELX*. *Acta Cryst.*, **A64**, 112–122.

Van der Heyden, A. & Edgecombe, D.R. (1990): Silver-lead-zinc deposit at South Mine, Broken Hill, *in* Geology of the mineral deposits of Australia and Papua New Guinea. Hughes, F.E., ed. Australasian Institute of Mining and Metallurgy. Monograph, Melbourne, **14**, 1073–1077.

Yvon, K., Jeitschko, W., Parthé, E. (1977): LAZY PULVERIX, a computer program, for calculating X-ray and neutron diffraction powder patterns. *J. Appl. Crystallogr.*, **10**, 73–74.

Received 2 August 2017
Modified version received 2 November 2017
Accepted 14 November 2017